Proc. Natl. Acad. Sci. USA
Vol. 86, pp. 6488–6492, September 1989
Biochemistry

Mammalian multidrug-resistance gene: Correlation of exon organization with structural domains and duplication of an ancestral gene

(gene structure/nucleotide-binding sites)

MARTINE RAYMOND AND PHILIPPE GROS*

Department of Biochemistry, McGill University, Montreal, Canada H3G 1Y6

Communicated by Phillip A. Sharp, May 15, 1989

ABSTRACT **Analysis of the nucleotide and deduced amino acid sequences of the biologically active mouse *mdr1* cDNA clone indicates that the protein is formed by two highly homologous halves, each containing six putative transmembrane domains and a nucleotide-binding site. The duplicated unit shows high sequence homology to the proposed energy-coupling subunit of bacterial periplasmic transport proteins. We have cloned and characterized the mouse *mdr1* gene and have analyzed the genomic organization of the two homologous halves forming the mdr1 protein. The gene spans 68 kilobases, is split into 28 exons, and the two homologous halves are encoded by 14 and 13 exons. The transcriptional initiation site of the gene has been mapped and putative TATA and consensus CAAT sequences have been found at positions −27 and −83, respectively. Discrete structural domains of the mdr1 protein are encoded by separate exons: Ten of the 12 putative transmembrane domains are encoded by individual exons and the two nucleotide-binding sites are each encoded by three exons. The exon/intron organization of the gene is conserved in the two highly homologous regions encoding the nucleotide-binding sites. The conservation of certain pairs of introns, together with the high degree of sequence homology, indicate that the mouse *mdr1* gene originated from the duplication of an intron-containing ancestral gene.**

The emergence of multidrug resistance in cultured cells is frequently associated with the amplification and overexpression of a small family of genes, named *mdr* or *pgp*, which encode P-glycoproteins (1–3). The gene family contains three members in rodents and two members in humans (4). We have isolated full-length cDNA clones for three closely related mouse *mdr* genes, *mdr1*(5), *mdr2* (6), and *mdr3* (A. Devault and P.G., unpublished data). The *mdr1* cDNA was shown to confer multidrug resistance when introduced and overexpressed in otherwise drug-sensitive cells (7). Analysis of the nucleotide and predicted amino acid sequences of this clone suggests that the mdr1 protein is a membrane glycoprotein formed by the duplication of a structural unit containing three putative transmembrane (TM) loops and a nucleotide-binding (NB) fold (5). This unit is highly homologous to the proposed energy-coupling subunit of several bacterial periplasmic transport systems, particularly *HlyB*, which participates in the outward transport of hemolysin in *Escherichia coli* (5, 8). These characteristic features have also been described for mouse *mdr2* and *mdr3* and for cloned members of the corresponding human (9, 10) and hamster (11) gene families. It has been proposed that the ancestor of the mammalian *mdr* gene originated from a duplication event and that the mammalian duplicated unit along with its bacterial homologs themselves evolved from a common, or at least closely related, ancestor. Elucidating the genomic organization of the mouse *mdr1* gene would give us the unique opportunity to analyze the evolutionary pathway of a mammalian gene that shares considerable sequence homology and, possibly, common ancestral origins with a group of bacterial genes that participate in related yet distinct transport events.

Drug transport studies in multidrug-resistant cell lines (12–14) together with the observed high degree of sequence homology to bacterial periplasmic transport genes (5) have led to the proposition that the biologically active *mdr1* gene encodes an ATP-driven drug efflux pump (5, 15). Although the function of individual *mdr* genes in normal cell physiology is not known, their level of expression is tightly regulated in a tissue-specific fashion. Detectable levels of mouse *mdr1* mRNA are observed mainly in kidney, placenta, heart, and adrenals, with the highest levels of expression appearing in endometrial glands of the uterus, late during pregnancy (16, 17). Also, it appears that increased *mdr* gene expression without gene amplification is associated with low levels of drug resistance in cultured cells (18, 19). Therefore, the isolation of genomic sequences overlapping the *mdr1* gene would allow the analysis of putative cis- and trans-acting elements participating in the regulation of *mdr1* gene expression in normal tissue and in drug-resistant tumor cells. This report describes the cloning and characterization of a complete mammalian *mdr* gene.† Our results indicate that the gene contains 28 exons, most of them encoding discrete structural domains of the protein, and suggest that *mdr1* was created by duplication of an intron-containing ancestral gene. Results are discussed with respect to the structural organization and evolutionary origin of the *mdr1* gene.

MATERIALS AND METHODS

Cell Culture. Mouse multidrug-resistant LTA 42.2-5 cells (from C. P. Stanners, McGill University, Montreal) were grown in α-MEM minimal essential medium and L1210DN cells (from J. Croop, MIT, Cambridge, MA) were grown in RPMI 1640 medium (GIBCO), both media were supplemented with 10% fetal calf serum and 2 mM L-glutamine. The medium for colchicine-selected LTA 42.2-5 cells contained colchicine (Sigma) at 5 μg/ml and the medium for daunomycin-selected L1210DN cells contained Adriamycin (Adria Laboratories) at 0.1 μg/ml.

Construction and Screening of Genomic Libraries. The construction and screening of genomic libraries were performed essentially as described (1). Briefly, high molecular

The publication costs of this article were defrayed in part by page charge payment. This article must therefore be hereby marked "*advertisement*" in accordance with 18 U.S.C. §1734 solely to indicate this fact.

Abbreviations: TM, transmembrane; NB, nucleotide binding; nt, nucleotide(s).

*To whom reprint requests should be addressed.

†This sequence has been deposited in the GenBank data base (accession no. J03398).

weight genomic DNA from L1210DN or LTA 42.2-5 cells was partially digested with *Sau*3A and size-selected on a NaCl gradient. L1210DN DNA was cloned into the *Bam*HI site of the λ EMBL3 vector and LTA 42.2-5 DNA was cloned into the *Bam*HI site of the cosmid vector pSAE. The ^{32}P-labeled full-length mouse *mdr1* cDNA clone λDR11 (5) was used as a probe for the detection of genomic clones.

DNA Sequencing. Exon-containing restriction fragments of genomic clones were identified by hybridization to cDNA and enzymatically sequenced by the chain-termination method of Sanger *et al.* (20).

S1 Nuclease Mapping. A 147-base-pair (bp) *Hpa* II genomic restriction fragment, spanning the 5′ end of the *mdr1* mRNA, was ^{32}P-labeled at both extremities with T4 polynucleotide kinase (Pharmacia), denatured in 50% formamide/0.5 M NaCl/40 mM Pipes, pH 6.4/1 mM Na_2EDTA and hybridized for 16 hr at 52°C to 20 μg of RNA that had been prepared from either sensitive or multidrug-resistant mouse cell lines (21). The DNA·RNA hybrids were then treated with S1 nuclease (Sigma) and analyzed on an 8% polyacrylamide gel containing 7 M urea.

RESULTS AND DISCUSSION

Structure of the *mdr1* Gene. The mouse *mdr1* cDNA clone (5) was used as hybridization probe to identify mouse *mdr1* genomic clones in bacteriophage and cosmid libraries constructed with genomic DNA from two independently derived multidrug-resistant mouse cell lines that show *mdr* gene amplification (L1210DN and LTA-42.2). A restriction map of the 90-kilobase (kb) genomic DNA domain encompassed by the inserts of six cosmid and three bacteriophage clones is shown in Fig. 1. The integrity of the cloned *mdr1* fragments was verified by comparing Southern blots of genomic DNA from drug-sensitive and -resistant cells probed with subfragments of the cloned domain (data not shown). The nucleotide sequence of the exons was found to be identical to that of the *mdr1* cDNA previously cloned from a drug-sensitive cell (5). Although the presence of discrete mutations or small deletions/additions within intron sequences cannot be formally excluded, our results indicate that multidrug resistance in the highly drug-resistant LTA-42.2 cells, used to construct the cosmid library, is caused by direct amplification and overexpression of an otherwise unmodified *mdr1* gene. This is in agreement with our previous demonstration that a full-length *mdr1* cDNA clone, isolated from drug-sensitive cells, can confer multidrug resistance in transfection experiments (7).

Exon/intron boundaries were established by DNA sequence comparison of cDNA and genomic subclones (Table 1). All splice donor and acceptor sites conform to the GT–AG rule and agree well with the consensus sequence compiled for the exon/intron boundaries of other genes (22). The schematic map (Fig. 1) and detailed exon/intron organization of the *mdr1* gene (Table 1) show that the gene spans 68 kb of genomic DNA consisting of 64 kb of intervening sequences and 4.3 kb of coding sequences. The gene is interrupted by 27 introns ranging in size from 90 bp to 8 kbp, while the length of the 28 exons varies from 49 to 559 bp (average size, 155 bp).

Analysis of the predicted amino acid sequence of the mdr1 protein identifies a series of 12 hydrophobic segments designated as TM domains and two putative NB folds (5, 23) similar to those described for several ATPases (23). A

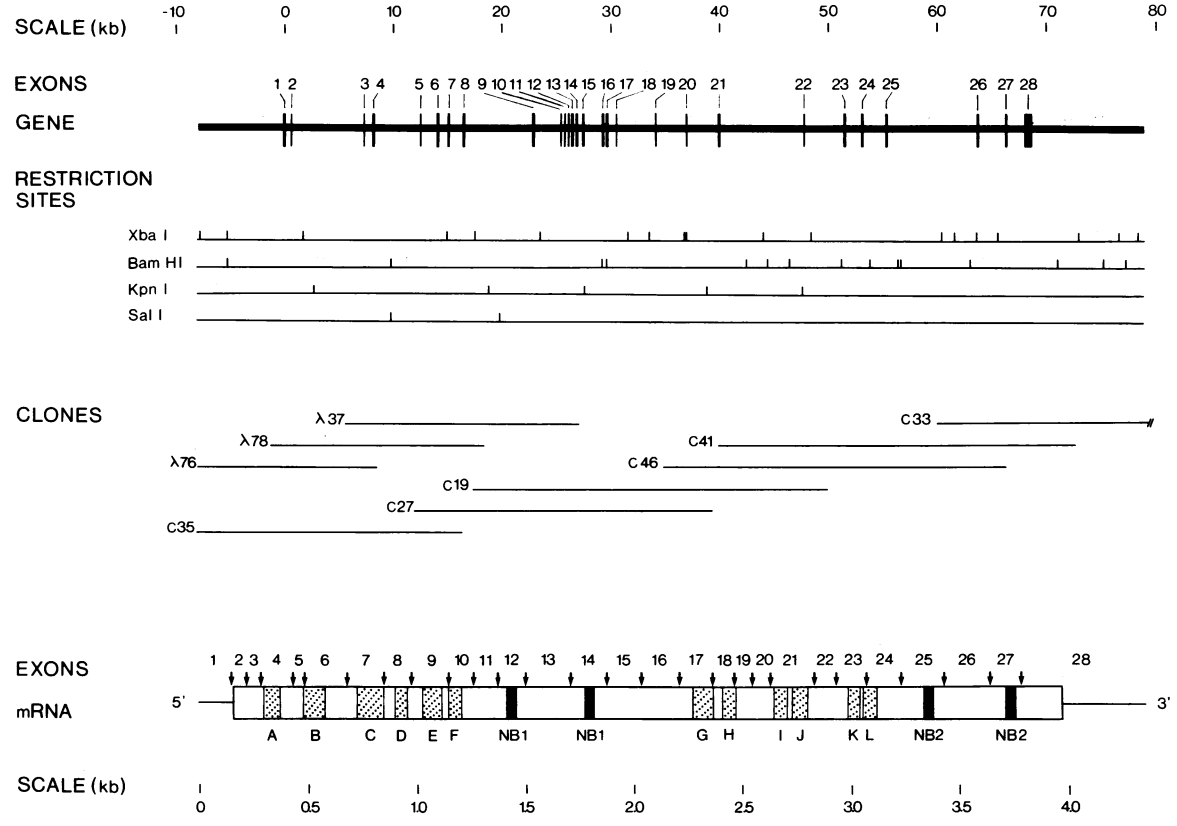

FIG. 1. Physical map of the mouse *mdr1* gene. (*Top*) The structure of the gene is schematically represented. Exons are represented by solid boxes (numbered 1–28) and intervening and flanking sequences are shown by a thick connecting line. The direction of transcription is from left to right. The scale (every 10 kb) is drawn above the gene. Recognition sites for restriction enzymes *Xba* I, *Bam*HI, *Kpn* I, and *Sal* I are given below. (*Middle*) Representative λ and cosmid clones are shown. (*Bottom*) Mouse *mdr1* mRNA. The boxed region indicates the coding sequences and the thin lines show the 5′ and 3′ untranslated regions. Stippled boxes (A–L) correspond to the 12 putative transmembrane segments and solid boxes (NB1 and NB2) show the positions of the two NB site consensus sequences. Arrows (numbered 1–27) identify intervening sequences in the precursor mRNA. The scale (every 0.5 kb) is shown below.

Table 1. Exon–intron organization of the mouse *mdr1* gene

Exon number	Exon position in mRNA	5′ donor	3′ acceptor
1	1–147	CGT GAG:gt . . .	ag:GTG GTG
2	148–218	AAG AG:gt . . .	ag:T AAA
3	219–267	GGG ATG:gt . . .	ag:TTT CGC
4	268–430	CAA A:gt . . .	ag:GT GGA
5	431–488	GCC AT:gt . . .	ag:A TAC
6	489–680	ACA GA:gt . . .	ag:T GAT
7	681–852	GCA AAG:gt . . .	ag:GTA TTG
8	853–977	GAA AG:gt . . .	ag:G TAC
9	978–1149	CTT ACT:gt . . .	ag:GTC TTC
10	1150–1263	GAT AAC:gt . . .	ag:GAG CCA
11	1264–1374	GTT CAG:gt . . .	ag:ATC TTG
12	1375–1500	GGC GTG:gt . . .	ag:GTC AGT
13	1501–1704	CCC CAC:gt . . .	ag:CAA TTT
14	1705–1875	GAT AAG:gt . . .	ag:GCT AGA
15	1876–2037	ACA CAG:gt . . .	ag:ACT AGA
16	2038–2211	GCT GTG:gt . . .	ag:GAT GAA
17	2212–2358	GTA GGG:gt . . .	ag:GTT TTT
18	2359–2466	TTT CAG:gt . . .	ag:GGC TTC
19	2467–2544	AGA CAG:gt . . .	ag:GAT ATA
20	2545–2628	AAA GGG:gt . . .	ag:GCG ATG
21	2629–2832	GGG AAG:gt . . .	ag:ATT GCT
22	2833–2933	TAC AG:gt . . .	ag:A AAT
23	2934–3074	ATG TT:gt . . .	ag:G GTA
24	3075–3231	AAG CCT:gt . . .	ag:ACT CTG
25	3232–3429	TCA GTG:gt . . .	ag:TTT CTA
26	3430–3636	CCT GAT:gt . . .	ag:AAA TAC
27	3637–3783	GAA AAG:gt . . .	ag:GTT GTC
28	3784–4342		

Exons are numbered from 5′ to 3′ in the direction of transcription. Exon sequences are in capital letters; introns are in lowercase letters.

projection of the position of the introns on the *mdr1* mRNA and the predicted structural features of the corresponding protein are shown in Fig. 1 (*Lower*). Exon 1 encodes the first 147 untranslated nucleotides at the 5′ end. Exon 2 contains the ATG translation initiation codon preceded by 6 untranslated nucleotides and encodes the first 21 amino acid residues. The 12 predicted TM domains, designated A–L in Fig. 1, are encoded by 11 separate exons, with the exception of domains I and J, which are both encoded by exon 21. Interestingly, 7 introns (nos. 3, 5, 7, 9, 17, 18, and 20) are each positioned at the border of a predicted TM domain, in agreement with the previous observation that introns often mark turns or edges in protein secondary structure (24). Each putative NB fold of the mdr1 protein is encoded by 3 discrete exons: exons 12, 13, and 14 in the 5′ half of the gene versus exons 25, 26, and 27 in the 3′ half. Exons 12 and 25 encode the amino-terminal segment and exons 14 and 27 encode the carboxyl-terminal segment of the NB folds. Exons 13 and 26 encode the protein segment connecting the amino- and carboxyl-terminal halves of each NB fold. Exon 28 encodes the remaining 66 amino acids at the carboxyl terminus of the protein and the 361 nucleotides of the 3′ untranslated region of the mRNA. Recently, the organization of seven carboxyl-terminus exons of three partial *pgp/mdr* hamster genes was elucidated (4) and shows identical intron/exon arrangement to that reported here for mouse *mdr1*.

These results indicate that a strong correlation exists in *mdr1* between the exon/intron arrangement of the gene and predicted structural domains of the protein. The specific positioning of introns at the boundaries of structural domains of complex proteins has been reported for several genes including immunoglobulin heavy chain (25), rhodopsin (26), and low density lipoprotein receptor (27). As proposed for these genes, the primordial *mdr* gene may have been assembled through the association of discrete exons by evolutionary mechanisms such as exon shuffling (28). Since conservation of the exon/intron structure of NB domains of three genes encoding NAD-binding proteins has been reported (24), we have compared the exon/intron organization of other eukaryotic genes, known to contain the NB consensus sequence, with that of the *mdr1* gene. We have found amino acid sequence homology (36%), similar intron positioning, and similar length (57 vs. 63 residues) of exon 14 of the *mdr1* gene and exon 4 of the rabbit muscle phosphofructokinase gene (29). The mammalian phosphofructokinase has evolved by duplication of a bacterial ancestor (29), binds ATP (30), and the protein domain encoded by exon 4 contains the carboxyl part of a NB fold (29). Also, exon 13 of *mdr1* shares amino acid sequence homology (35%), similar intron positioning, and length (42 vs. 40 residues) with exon 4 of another ATP-binding protein, the mitochondrial ATP synthase gene from *Nicotiana plumbaginifolia* (31). These observations suggest that these exons share a common ancestor, implicated in nucleotide binding, which would have been recruited in the formation of these unrelated genes.

Mapping of the Transcription Start Site and Sequence Analysis of the Promoter Region. Total RNA from either sensitive or multidrug-resistant mouse cell lines was used to protect a 147-bp double-stranded *Hpa* II genomic DNA fragment in S1 nuclease protection experiments (see Fig. 3; from −15 to +132 on the complementary strand). Regardless of which RNA preparation was used to protect the probe, the S1 nuclease digestion product was consistently a fragment of 132 nucleotides (nt) (Fig. 2). The 147-nt fragment present in all lanes corresponds to residual undigested probe as shown in lane A. These results imply that the transcription initiation site is located at the cytosine residue numbered +1 (Fig. 3) and that the *mdr1* mRNA, with a 5′ untranslated leader of 147 nt, is 4342 nt long. The amount of probe protected from S1 nuclease digestion (band intensity in the autoradiograph) is proportional to the amount of specific *mdr1* mRNA expressed in the drug-sensitive and -resistant lines tested. It is worth noting that, unlike the human *mdr1* gene in which two

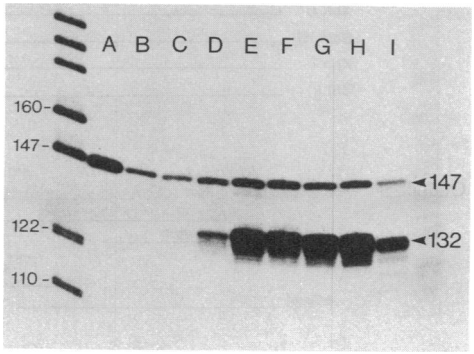

FIG. 2. Determination of the site of initiation of transcription by S1 nuclease mapping. A 147-bp *Hpa* II genomic fragment (−17 to +130) was end-labeled at both extremities with ^{32}P and hybridized to the different RNAs listed below. Single-stranded DNA was then digested with different concentrations of S1 nuclease and products were analyzed on a denaturing polyacrylamide gel. The 147-bp band is the incompletely digested probe and the 132-bp band corresponds to the protected fragment. Each lane contains the 147-bp labeled fragment and no RNA (lane A), tRNA (lane B), total RNA of drug-sensitive LTA cells (lane C), total RNA of drug-resistant L1210DN cells (lane D), total RNA of drug-resistant LTA 42.2-5 cells (lanes E, G, H, and I), and polyadenylylated RNA from LTA 42.2-5 cells (lane F). Lanes B–F were treated with 30 units of S1 nuclease and lanes G–I were treated with 60, 125, and 500 units. The size of the protected fragment (bp) has been deduced from end-labeled pBR322/*Hpa* II fragments (left lane) and from a sequencing ladder (data not shown).

```
                                                                    -51
...tgccccaatcccacccaccaggctgattggctgccgg
                                                                     10
gccttagggcggccgctggcatctattttaatccgggggcccgaggaagccCTCTGGCTCC
                                                                     70
TTCCCGCAGTGGCTCTTGAAGCCGTAAGAGGCTGAGGCCGCTGCTTCCATCTTCTGAGGT
                                                                    130
TCCGCTCAACTCAGAGCTACTTCCAAATTCTACATCTTGGCTGACTTTGCGAAGGAAACC
                                                                    610
CGGAGGTGGCACGTGAGgtaggcag---431bp---tcctcagGTGGTGATGGAGTTTGA
                                                                    667
AGAGAACCTTAAGGGAAGAGCAGACAAGAACTTCTCGAAGATGGGCAAAAAGAGgta...
```

FIG. 3. Nucleotide sequence of the promoter region. The sequence shown has the same polarity as the mRNA. Nucleotides are numbered with respect to the site of initiation of transcription. Exons are in capital letters and introns and the promoter region are in lowercase letters. The putative TATA sequence and consensus CAAT sequence are underlined. The transcription start site is marked by a solid arrow; the translation start site is identified by an open arrow.

alternate transcription initiation sites appear to be used in certain drug-resistant lines (32), the mouse *mdr1* gene is transcribed from a unique initiation site in the drug-resistant lines analyzed. The 5′ end of the *mdr1* gene, as determined by S1 nuclease mapping, is contained within a 1.4-kb *Eco*RI genomic fragment (clone c35; Fig. 1), whose partial sequence is presented in Fig. 3. The 5′-flanking region shows sequence elements likely to represent eukaryotic pol II promoter elements (33): a TATA like sequence, TATTTAAT from −27 to −19, a GC box, GGGCGG from −47 to −39, and a canonical CAAT box, CCAATC from −83 to −78. In mice, the highest levels of *mdr1* gene expression are detected in the pregnant uterus at 16 days of gestation, in the adrenals, and, to a lesser degree, in the kidneys and heart (16). In cell lines showing low levels of drug resistance, overexpression of *mdr* genes often occurs without gene amplification (refs. 18 and 19; unpublished data). The isolation of genomic sequences spanning the 5′ upstream regulatory region of the *mdr1* gene will allow us to study the mechanisms and cellular factors implicated in the tissue-specific activation of this gene in normal tissues and in multidrug-resistant cells.

Duplication of the *mdr1* Gene. The two homologous halves of *mdr1* show 54% nucleotide sequence identity (65% in NB folds, residues 419–628 and 1061–1272; 48% in TM domains, residues 113–418 and 752–1060) translating into 43% identical residues (63% in NB folds; 30% in TM domains) with an additional 27% conserved substitutions (20% in NB folds; 32% in TM domains) for a total of 70% homology (83% in NB folds; 62% in TM domains). We have positioned the introns on an amino acid alignment of the two homologous halves of the protein and analyzed the exon/intron organization (Fig. 4). The 5′ and 3′ halves of the protein are each encoded by 14 and 13 exons, respectively. Intron 15 occurs roughly at the border of the duplicated segment, dividing the gene in two unequal halves (≈28 kb for the 5′ half and ≈40 kb for the 3′ half).

Amino acid sequence alignment between the duplicated halves of the mdr1 protein (Fig. 4) shows a gradient of sequence conservation ranging from weak homology, near the amino termini, to near identity in the carboxyl termini (NB folds). The extent of conservation of the genomic exon/intron structure appears to parallel the degree of amino acid sequence homology between the duplicated halves of the protein. The exon/intron organization of genomic regions encoding the sequence divergent segments corresponding to the TM domains of the mdr1 protein is different in each half of the gene, only introns 9 and 23 being located 1 nt apart. Although the position of introns within these regions is different in both halves of the molecule, they nevertheless

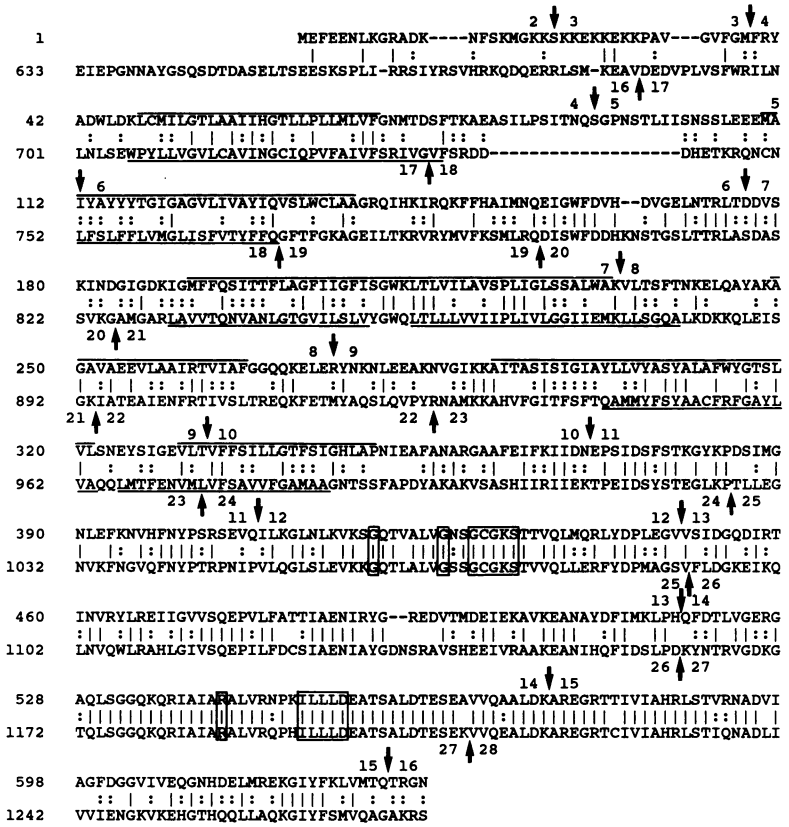

FIG. 4. Internal duplication of the mdr1 protein and intron boundaries. Amino acid sequences from the amino-terminal (residues 1–632) and carboxyl-terminal (residues 633–1276) halves of the mdr1 protein are aligned. The standard single-letter amino acid code is used. The amino acid number is on the left of each line. Identities or highly conservative substitutions are indicated by vertical lines or colons, respectively. Predicted transmembrane segments are indicated by horizontal lines and consensus sequences for the NB sites are boxed. Arrows indicate the location of introns and are flanked by the corresponding exon numbers.

delineate 10 exons, each encoding individual TM domains. Within the highly homologous regions encoding the NB folds, the position of the intron boundaries appears to be conserved, particularly intron pairs 12/25 and 13/26, which precisely delimit two homologous exons (exon 13, 68 residues; exon 26, 69 residues). The position of the splice site for the latter pair has been preserved at the nucleotide level.

Clarification of the genomic organization of *mdr1* allows us to speculate on possible evolutionary mechanisms that may be responsible for the creation of the present day *mdr1* gene. First, the gene could have evolved from the duplication of an ancestor gene already containing approximately half the number of introns of the mouse gene. The observation that both halves of the protein are encoded by a similar number of exons—14 vs. 13—and that at least one intron pair (nos. 13 and 26) is located at exactly the same position within the NB folds would support this proposal. However, it is difficult to envision a molecular mechanism responsible for the movement of duplicated introns within the gene, especially those delineating homologous exons encoding the highly conserved NB domains (compare position of introns 14 and 27). Alternatively, an ancestral *mdr* gene containing a very limited set of introns would have duplicated and subsequently acquired additional introns now present in the mouse *mdr1* gene. This subsequent evolution could have happened within a single internally duplicated gene or, independently, in two separate transcription units prior to fusion. This model would account for the lack of precise conservation of exon/intron boundaries that should be expected from the duplication of an ancestral gene containing a complete set of introns. In conclusion, the preservation of certain pairs of introns and the high degree of sequence homology between the two halves of *mdr1* clearly point at the duplication of an ancestral gene containing introns. However, the precise number of introns in this ancestor cannot be ascertained at this point. Characterization of *mdr* genes from lower eukaryotes should help to determine the specific pattern of intron gain or loss that might have occurred in the evolution of the mouse gene.

The authors thank Drs. C. P. Stanners and J. Croop for the gift of cell lines LTA42.2 and L1210DN, respectively. We thank Drs. C. P. Stanners, W. Mushynski, and D. Housman for critical reading of this manuscript, and P. Chipman for secretarial assistance. This work was supported by grants from the Canadian Medical Research Council and National Cancer Institute (to P.G.). M.R. is suported by a scholarship from the Medical Research Council of Canada.

1. Gros, P., Croop, J., Varshavsky, A. & Housman, D. E. (1986) *Proc. Natl. Acad. Sci. USA* **83,** 337–341.
2. Roninson, I. B., Chin, J. E., Choi, K., Gros, P., Housman, D. E., Fojo, A., Shen, D., Gottesman, M. M. & Pastan, I. (1986) *Proc. Natl. Acad. Sci. USA* **83,** 4538–4542.
3. Riordan, J. R., Deuchars, K., Kartner, N., Alon, N., Trent, J. & Ling, V. (1985) *Nature (London)* **316,** 817–819.
4. Ng, W. F., Sarangi, F., Zastawny, R. L., Veinot-Drebot, L. & Ling, V. (1989) *Mol. Cell. Biol.* **9,** 1224–1232.
5. Gros, P., Croop, J. & Housman, D. E. (1986) *Cell* **47,** 371–390.
6. Gros, P., Raymond, M., Bell, J. & Housman, D. E. (1988) *Mol. Cell. Biol.* **8,** 2770–2778.
7. Gros, P., Ben-Neriah, Y., Croop, J. & Housman, D. E. (1986) *Nature (London)* **323,** 728–731.
8. Felmlee, T., Pellett, S. & Welch, R. A. (1985) *J. Bacteriol.* **163,** 94–105.
9. Chen, C., Chin, J. E., Ueda, K., Clark, D. P., Pastan, I., Gottesman, M. M. & Roninson, I. B. (1986) *Cell* **47,** 371–389.
10. Van der Bliek, A. M., Baas, F., Ten Houte de Lange, T., Kooiman, P. M., Van der Velde-Koerts, T. & Borst, P. (1987) *EMBO J.* **6,** 3325–3331.
11. Endicot, J. A., Juranka, P. F., Sarangi, F., Gerlach, J. H., Deuchars, K. L. & Ling, V. (1987) *Mol. Cell. Biol.* **7,** 4075–4081.
12. Dana, K. (1973) *Biochim. Biophys. Acta* **323,** 446–483.
13. Skovsgaard, T. (1978) *Cancer Res.* **39,** 4722–4727.
14. Fojo, A., Akiyama, S., Gottesman, M. M. & Pastan, I. (1985) *Cancer Res.* **45,** 3002–3007.
15. Croop, J., Gros, P. & Housman, D. (1988) *J. Clin. Invest.* **81,** 1303–1309.
16. Croop, J. M., Raymond, M., Haber, D., Devault, A., Arceci, R. J., Gros, P. & Housman, D. E. (1989) *Mol. Cell. Biol.* **9,** 1346–1350.
17. Arceci, R. J., Croop, J. M., Horwitz, S. B. & Housman, D. (1988) *Proc. Natl. Acad. Sci. USA* **85,** 4350–4353.
18. Shen, D.-W., Fojo, A., Chin, J. E., Roninson, I., Richert, N., Pastan, I. & Gottesman, M. M. (1986) *Science* **232,** 643–645.
19. Lemontt, J. F., Azzaria, M. & Gros, P. (1988) *Cancer Res.* **48,** 6348–6353.
20. Sanger, F., Nicklen, S. & Coulson, A. R. (1977) *Proc. Natl. Acad. Sci. USA* **74,** 5463–5467.
21. Chirgwin, J. M., Przybyla, A. A., MacDonald, R. J. & Rutter, W. J. (1979) *Biochemistry* **18,** 5294–5306.
22. Mount, S. M. (1982) *Nucleic Acids Res.* **10,** 459–472.
23. Walker, J. E., Saraste, M., Runswich, M. J. & Gay, N. J. (1982) *EMBO J.* **1,** 945–951.
24. Michelson, A. M., Blake, C. F., Evans, S. T. & Orkin, S. H. (1985) *Proc. Natl. Acad. Sci. USA* **82,** 6965–6969.
25. Sakano, H., Rogers, J. H., Hippi, K., Brock, C., Traunecker, A., Maki, R., Wall, R. & Tonegawa, S. (1979) *Nature (London)* **277,** 627–633.
26. Nathans, J., & Hogness, D. S. (1983) *Cell* **34,** 807–814.
27. Sudhof, T. C., Goldstein, J. L., Brown, M. S. & Russell, D. W. (1985) *Science* **228,** 815–822.
28. Gilbert, W. (1978) *Nature (London)* **271,** 501–505.
29. Lee, C.-P., Kao, M.-C., French, B. A., Putney, S. D. & Chang, S. H. (1987) *J. Biol. Chem.* **262,** 4195–4199.
30. Evans, P. R. & Hudson, P. J. (1979) *Nature (London)* **279,** 500–504.
31. Boutry, M. & Chua, N.-H. (1985) *EMBO J.* **4,** 2159–2165.
32. Ueda, K., Pastan, I. & Gottesman, M. M. (1987) *J. Biol. Chem.* **262,** 17432–17436.
33. Bucher, P. & Trifonov, E. N. (1986) *Nucleic Acids Res.* **14,** 10009–10026.